applied sciences

MDPI

Article

Model Test Analysis of Subsurface Cavity and Ground Collapse Due to Broken Pipe Leakage

Fei Tan [1], Wufeiyu Tan [1], Feifei Yan [1], Xin Qi [1,2,*], Qinghua Li [2] and Zhikai Hong [1]

[1] Faculty of Engineering, China University of Geosciences, Wuhan 430074, China
[2] Wuhan Center, China Geological Survey, Wuhan 430205, China
* Correspondence: qx_cdut@126.com

Abstract: Urban ground collapse is a common geological disaster characterized by its invisible nature, particularly in China, and results in significant socioeconomic losses and even loss of life. Underground pipeline breakage is the most common factor leading to urban ground collapses. Hence, it is essential to study how different types of pipeline breakages initiate the collapse mechanism. In this study, an indoor model test was conducted to directly observe the process of collapse due to broken pipe leakage. A broken pipe was put into a model box and tested by an experimental device. The results showed that among the different pipeline breakage types, vertical damage had the greatest influence on the degree of cavity development and ground collapse. Similarities were observed in the patterns of cavity evolution development and the extent of ground collapse as well, further revealing the significance of the cavity evolution process in predicting ground collapses.

Keywords: urban ground collapse; underground cavity; pipeline breakage type; indoor model test; collapse mechanism

Citation: Tan, F.; Tan, W.; Yan, F.; Qi, X.; Li, Q.; Hong, Z. Model Test Analysis of Subsurface Cavity and Ground Collapse Due to Broken Pipe Leakage. *Appl. Sci.* **2022**, *12*, 13017. https://doi.org/10.3390/app122413017

Academic Editor: Arcady Dyskin

Received: 15 November 2022
Accepted: 16 December 2022
Published: 19 December 2022

1. Introduction

Following various reforms and the opening up of the economy, China has been on a high growth trajectory in various fields. With the increase in population density and demand for higher quality of life, the intensity of development above and below ground has increased, and the load on municipal pipelines and road traffic has been high, consequently exacerbating the phenomenon of urban ground collapse, which is closely related to human activities. In recent years, urban ground collapses have become one of the major geological disasters threatening urban development. A ground collapse can be characterized by concealment, suddenness, mass occurrence, and serious damage; they can cause significant casualties and economic losses, particularly in cities. The largest cities have the highest frequency of ground collapse accidents, owing to their highly developed urbanization [1]. According to statistics, between 2007 and 2009 there were 277 road collapses in Beijing [2], with this number growing year by year. More than 90 cases of ground collapses have occurred in Shanghai since 2003 [3], posing a great threat to urban traffic, civilian safety, and socioeconomic development.

An urban ground collapse can be divided into two types, natural and artificial, depending on the main cause of the collapse. Unlike a natural collapse, an artificial collapse tends to occur more rapidly and on a larger scale and to result in a greater extent of damage. Engineering construction is highly susceptible to urban ground collapse, such as subway excavation in Qingdao [4], gypsum mines in Xingtai [5] and the issue of potential ground collapse when drilling [6]. Similarly, in Bangkok, Thailand [7], Ho Chi Minh City, Vietnam [8], Indonesian cities [9], and Fars Province, Iran [10,11], it has been concluded that human activities such as groundwater extraction and underground infrastructure construction are the main causes of urban ground collapses.

Field investigations have shown that most urban ground collapses are directly associated with urban underground pipelines [12]. Ground collapse caused by pipeline breakage accounts for a large proportion of the artificial causes of urban ground collapse incidents. Hu et al. [13] conducted a statistical analysis of ground collapse cases in China, and pointed out that 55% of all collapse accidents were caused by pipeline breakage.

Due to the concealment of underground pipeline breakage, the process of water seepage and erosion and the impact on the ground are difficult to observe after the occurrence of breakage. In terms of the disaster mechanism of ground collapse caused by pipeline breakage, scholars have focused on the disaster-causing process of "pipeline breakage ⟶ soil erosion ⟶ cavity evolution ⟶ ground collapse". The disaster-causing mechanism has been studied from four aspects: type of pipeline breakages, hidden forms and causes, the loss process of water and soil interpenetration, and cavity evolution before ground collapse. Based on computer fluid dynamics (CFD) and discrete element method (DEM), Wang and Lu [14] used the flow–solid coupling method to explore the loss process of soil under the action of water flow. Similarly, Zhou et al. [15] adopted the CFD-DEM method to investigate the patterns of stratum deformation and foundation loss as well as typical particle flow processes. Ben-Mansour et al. [16] performed CFD simulations on pipe leaks of different sizes using a 3D turbulence model. Peche et al. [17] used the pipe flow simulator HYSTEM-EXTRAN coupled with the groundwater flow simulator OpenGeoSys to study the effects of pipe flow and duration on breakage. Lau et al. [18] proposed a method for estimating the location of pipeline seepage and leaks in conjunction with a ground penetrating radar (GPR) algorithm. Qi et al. [19] used numerical calculations to simulate the change in the cavity stability in the presence of pipe breakage. Al-Halbouni et al. [20] used DEM and PFC software to simulate cavity expansion by quasi-static stepwise material removal in the cavity expansion domains of different geometries at different depths. Rahnema et al. [21] combined the finite element model (FEM) and field data, and concluded that considering the results of both R- and P-wave analysis can efficiently identify cavities. Mirassi and Rahnema [22] compared the propagation mechanisms of the longitudinal (P), Rayleigh (R) and shear (S) waves, and found that low frequencies or passive methods should be used to detect deep cavity. Tang et al. [23] coupled a Darcy fluid model with a DEM approach to study the erosion process of the surrounding soil by a sewage pipe. Due to the suddenness and concealment of pipeline breakage and the complexity of the causative factors and mechanisms, most scholars have studied ground collapses induced by pipeline breakage through numerical simulations. The mechanism of ground collapse caused by pipeline breakage can often be more intuitively analyzed through physical model tests. In physical model experiments, dry sand is mostly used as the experimental overlaying soil for indoor tests in order to make the test effects more evident. Cui et al. [24] used a combination of numerical calculations and model tests to study the damage process in sandy soils due to pipeline seepage. Indiketiya et al. [25] used dry sand as the experimental material to study the formation and evolution of cavities after pipeline breakage through indoor tests. Nazari et al. [26] used sand to conduct physical experiments on the hydraulic characteristics of flow. Ali and Choi [27] used dry sand as the soil overlaying the pipe to study the surface settlement and collapse pattern after pipeline breakage, considering the soil type, water flow type, and breakage location in the pipe. However, field investigations on urban ground collapse accidents have shown that in addition to being prone to ground collapse accidents in sandy soils, ground collapses can occur in clay as well.

This study adopted an indoor model test method with a mixture of sand and clay as the experimental material, designed a semi-structural model box to visualize the deformation characteristics of the underground cavity, and used a 3D scanner to observe the ground collapse clearly and quantitatively. We tried to put PVC pipes with different types of breakage into the experimental model box. The examined types of pipe breakage include wall perforation, circumferential damage, and vertical damage. Then, we filled the experimental box with soil and pumped water into the pipe for testing. The influence patterns of pipe breakage on ground collapse were studied by varying the type and size of cracks induced in the pipe.

2. Testing Program

2.1. Testing Apparatus

The relevant parameters were selected based on the dimensional analysis method of the second theorem of similarity, and the similarity ratio between the experimental materials used in this model experiment and the actual prototype materials was set to 10. Figure 1 shows the test model box. It was a soil box with a length of 1 m, a width of 0.2 m and a height of 0.8 m. It was fixed and reinforced with a steel frame as the outer frame. For convenience of observation, the soil box was designed as a semi-structure and its body was made of transparent acrylic board. On the left and right sides of the model box at a height of 35 cm, a circular pipe with 5 cm in diameter was installed; then, the test pipe was inserted through the reserved holes on the left and right sides to simulate an underground pipeline. On the front of the model box, gridlines were drawn every 5 cm from a height of 20 to 60 cm to observe the cavity initiation and evolution processes.

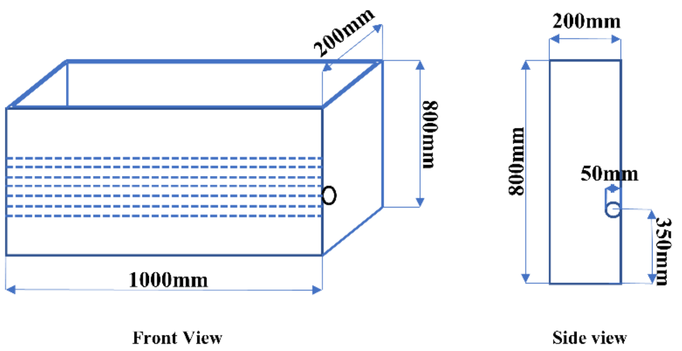

Figure 1. Schematic of the model box.

As shown in Figure 2, the indoor model test apparatus included a test model box, a water tank, a pressure pump, and a filtering water tank. Water could be circulated during the experiment using this apparatus, thereby saving water.

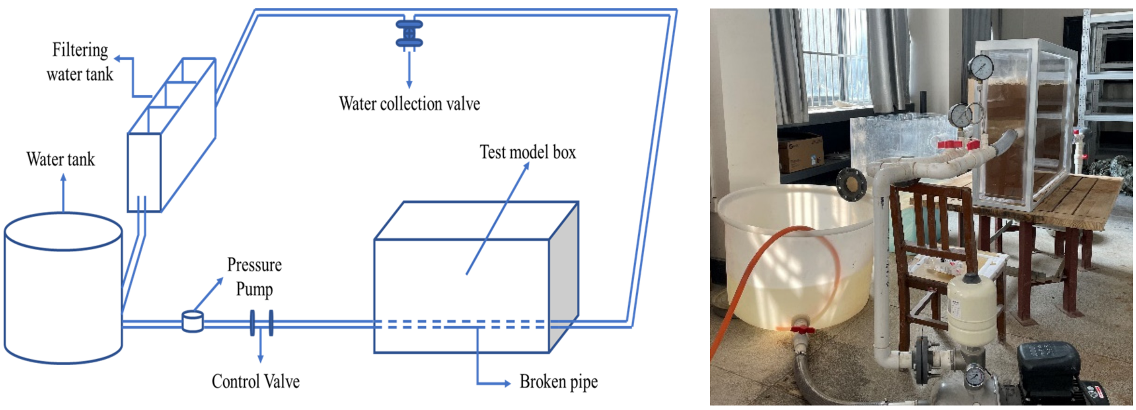

Figure 2. Experimental equipment.

For the development of an underground cavity caused by the pipeline breakage and ground collapse, measuring points were laid on the soil pressure box in the test, as shown in Figure 3. The soil pressure measurement system comprised three miniature soil pressure boxes with a range of 200 kPa, three miniature soil pressure boxes with a range of 500 kPa, and a data collection instrument. The soil pressure boxes were numbered 201#, 202#, 203#, 501#, 502#, and 503#. Taking the vertical centerline of the pipeline crack as the axis, miniature soil pressure boxes with vertical distances of 5 cm and 10 cm above the pipeline were symmetrically arranged; the horizontal spacing was 15 cm, and a miniature soil pressure boxes with a range of 500 kPa was placed on the horizontal plane of 5 cm. A 3D laser scanner was used to scan the ground at the beginning and end of the experiment, and the results were post-processed using Geomagic software.

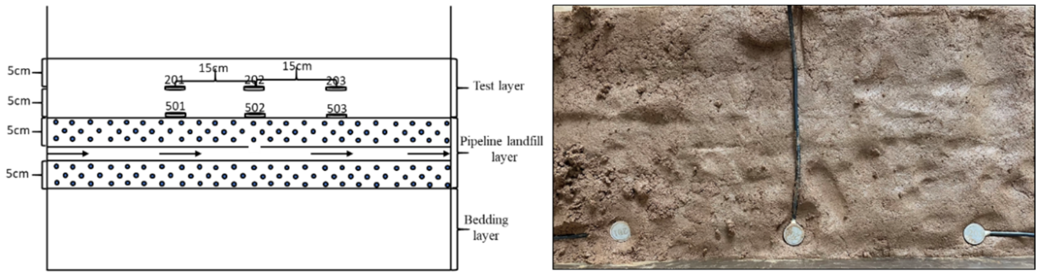

Figure 3. Arrangement of monitoring points.

2.2. Testing Material

Several previous testing materials were carefully studied. There are two main materials for model testing of ground collapse: (1) with dry sand as the experimental fill, the effect of the collapse process is evident; however, the soil cohesion in the actual situation is ignored; (2) with clay as the soil overlaying the pipeline, the cohesion of the actual material is considered; however, the experimental effect of the collapse process is not evident. Considering the experimental effect and actual situation, we used a soil mixture including both sand and clay as testing material. A mixture of sand and clay at a mass ratio of 2:1 was adopted as the soil overlaying the experimental pipeline.

Figure 4 shows the filling of the experimental materials in the model box, which can be divided into three parts. Part I was filled with a 250 mm-high cohesive soil as the bedding layer. Part II was filled with 100 mm-high sand as the pipe fill layer. In Part II, 50 mm of sand was first filled from the bottom of the pipe installation hole, the experimental pipeline was inserted, and the crack in the pipeline was adjusted to be upward and in the middle of the model box. Then, it was filled with a 50 mm-high sand. Part III was filled with a 100 mm-high sandy soil mixture as the overlaying soil above the pipe. The micropressure cells were placed in this layer based on the designed position and then buried. The experimental soil was added to the model box in nine layers using the falling rain method and the leveling method, with each layer being 50 mm in order to ensure adequate compaction.

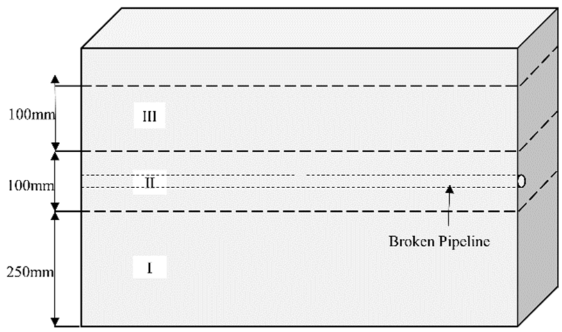

Figure 4. Model filling division.

2.3. Testing Procedure

Considering the complex and diverse forms of pipeline breakages observed in practice, three common types of pipeline breakages were studied: wall perforation, circumferential damage, and vertical damage. Based on these types, three different model tests (Figure 5) were set up to study the influence mechanism of underground cavity development and the degree of ground collapse under different sizes and types of cracks in the pipeline.

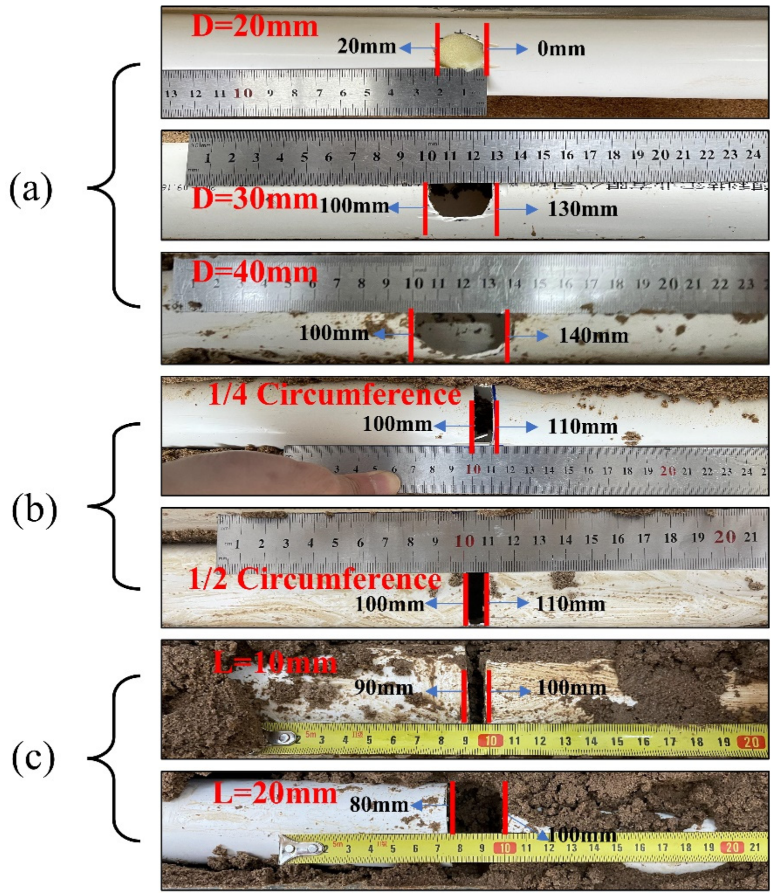

Figure 5. Types of experimental groups: (**a**) wall perforation group; (**b**) circumferential damage group; (**c**) vertical damage group (black fonts for scale reading).

Group 1: Pipe wall perforations. Circular cracks were created in the middle of the pipe of 20, 30, and 40 mm in diameter to study the effect of crack size on ground collapse.

Group 2: Circumferential damage. Circumferential damage tests were conducted by varying the size of the circumferential cracks to one quarter and half the value of the circumference, both 10 mm wide. Simulations were performed on two types of pipe water seepage conditions: surge leak (water gushing out from the defective point over an area no larger than one third of the pipe section) and spray leak (water spewing out from the defect point or when the area of the leaking water surface is greater than one third of the pipeline section).

Group 3: Vertical damage. Vertical damage tests were conducted with spacing sizes of 10 mm and 20 mm, with truncated pipes inserted from the ends of the pre-drilled holes in the sidewalls; the crack size was adjusted by controlling the distance between the ends. The different types of pipe leakage conditions helped simulate water erosion damage in different erosion areas.

The experimental pipe was placed based on the model filling procedure, and the pipe crack was set above. Subsequently, the experimental pipe was connected to the water pump and the filter water tank through a PVC hose. During the experiment, the water pump delivered water to the experimental pipeline at a constant pressure of 0.2 MPa. To simulate the peak and low-peak water consumptions observed in practice, the pump was operated for 1 min and stopped for 20 s.

3. Results and Discussion

3.1. Cavity Initiation and Evolution Processes

A circular crack 20 mm in diameter was used as an example to analyze the development process of the underground cavity; other groups had similar erosion development patterns of the pipe and soil structures. Figure 6 clearly shows the development of the underground cavity erosion under the hydraulic action of pipe leakage, which eventually causes the ground to collapse. This process can be divided into three stages.

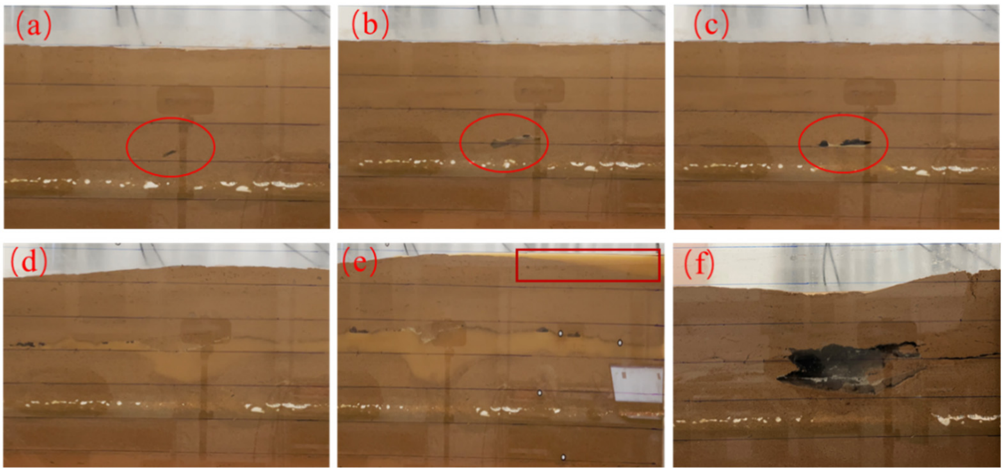

Figure 6. Evolution of an underground cavity formed by pipe seepage erosion from a circular crack 20 mm in diameter: (**a**) t = 60 s, first appearance of cavity; (**b**) t = 140 s, cavity becomes larger and stable; (**c**) t = 160 s, cavity shrinks after unloading; (**d**) t = 490 s, cavity expands suddenly; (**e**) t = 530 s, topping up the ground and water bursting onto the ground; (**f**) t = 560 s, ground collapse.

Stage 1 is the soil erosion stage. When the experiment was started, the pipe water flowed out from the crack and scoured the sand bedding layer around the pipe, gradually saturating the surrounding sand and forming an arch-shaped infiltration surface followed by the loss of sand particles with the pipe water under hydraulic action, and tiny fissures began to appear in the sand layer.

Stage 2 is the stable stage of cavity development. As the pipeline water continued to flow out and induce scouring, under constant hydraulic erosion, the sand layer was continuously hollowed out and lost. The cavity area gradually expanded to the sand layer and the pipeline overlying soil interface, and the weakly permeable experimental soil was equivalent to a waterproof layer.

(1) During the loading process, the seepage force of the flowing water could not cause effective erosion on the experimental soil, the scouring effect on the cavity walls was reduced, and the cavity was in a stable state.
(2) During the unloading process, the pressure of the flowing water on the cavity wall decreased, the experimental soil layer was lost, an increasing amount of soil around the cavity became loose, and the cavity shrunk.
(3) Reloading caused the cavity to expand under sudden pressure. During the expansion and shrinkage process, the structure of the cavity wall gradually deteriorated, and the flowing water gradually eroded the soil. The scale of the cavity was in a stable development state.

Stage 3 is the ground collapse stage. The scale of the cavity continues to develop during the continuous expansion and shrinkage process. When the supporting force of the cavity wall becomes lower than the scouring effect of the water flow, the pressure around the cavity changes suddenly (Figure 7).

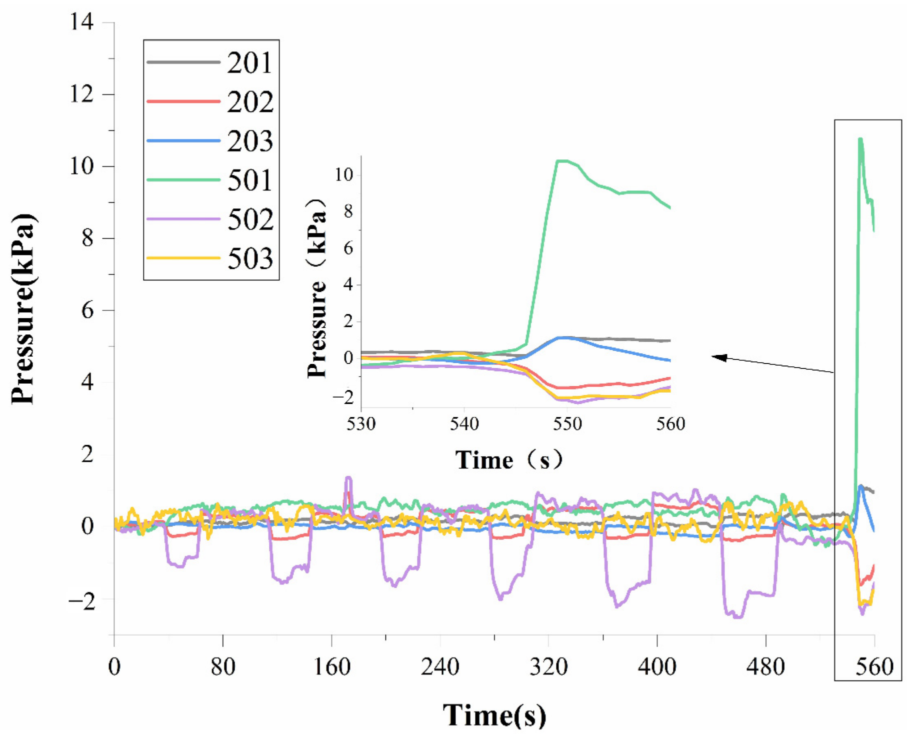

Figure 7. Pressure curves corresponding to each measurement point in a 20 mm-diameter circular crack.

(1) From 480 s onward, the pressure in the 502# and 202# pressure boxes directly above the crack exhibited the same waveform; however, there was a significant drop in the pressure, indicating that the cavity wall above had been damaged.
(2) Due to the direction of the water flow from left to right, the pressure in the 503# pressure box on the right side also decreased due to the pressure release from the cavity wall damage. The pressure in the 501# pressure box on the left side decreased; because the wall of the cavity above and on the right side was destroyed first, an increasing amount of soil around the cavity was lost, and the cavity gradually expanded, because of which the water flow formed a swirl on the left side and the pressure dropped after a sudden increase.
(3) The 201# and 203# pressure boxes were located on the left and right sides of the vertical plane of the upper crack, where the uplift of the ground surface caused the earth pressure to rise.

Finally, an elliptical cavity was formed, and the ground surface formed an area of settlement similar to an inverted triangle, with the ground surface sinking on the vertical surface of the pipe crack and rising on both sides, eventually forming a ground collapse.

Although each group of erosion processes had a similar development pattern, under different crack sizes the seepage force of the flowing water from the pipeline was different. Due to the three stages of cavity development in terms of time and extent, the impact of eventual ground collapses will be different.

From Table 1, it can be seen that:

(1) In the pipe wall perforation group with smaller cracks, the crack diameters were 20, 30, and 40 mm, though the cavity height hovered between 65 mm and 70 mm and the cavity width increased from 174 to 215 mm. As the crack size increased, the water flow from the pipe into the soil cavity increased, thereby increasing the seepage force of the flowing water on the soil; the underground cavity increased with the crack size, the area of the soil cavity continued to expand, and the underground cavity exhibited an oval shape (Figure 8a).

(2) In the experimental group of circumferential damage, the width and height of the 1/4 circumferential crack cavity was 490 mm and 40 mm respectively, while the width of the 1/2 circumferential crack cavity was only 154 mm; the height was 68 mm. The width and height of the cavity varied considerably in both the groups, and the soil cavity formed by soil erosion damage exhibited two different shapes (Figure 8b).

Table 1. Dimensions of cavity for different damage types.

Type of Cavity		Cavity Height (mm)	Cavity Width (mm)
Pipe wall perforation group	20 mm-diameter circular crack	66	174
	30 mm-diameter circular crack	70	190
	40 mm-diameter circular crack	65	215
Circumferential damage group	1/4 circumferential crack	40	490
	1/2 circumferential crack	68	154
Vertical damage group	1 cm vertical crack	59	280
	2 cm vertical crack	58	270

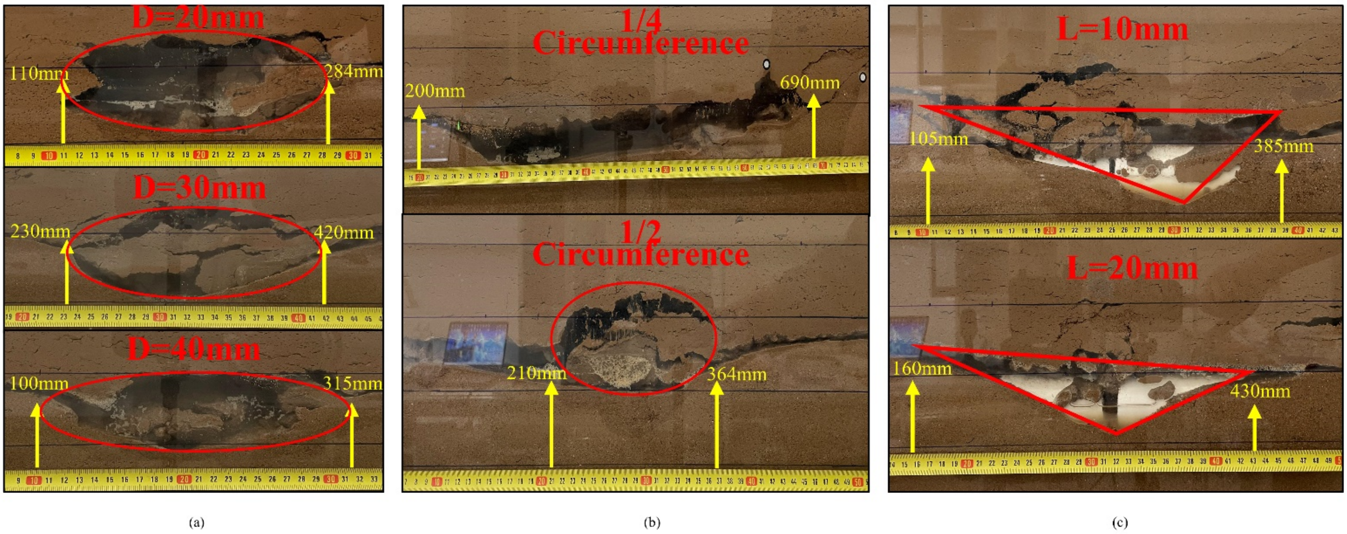

Figure 8. Soil cavity development: (**a**) wall perforation group; (**b**) circumferential damage group; (**c**) vertical damage group (yellow font for scale reading).

From the analysis of the pressure curve corresponding to Stage 3, the water flow in the pipeline from left to right caused the wall above the crack and the right side to be broken first. Therefore, when the supporting force of the left side wall was greater than the water flow pressure and when the right-side wall of the soil cavity was continuously damaged and extended, the cavity that was formed by the circular crack with a relatively small size of one quarter the circumference elongated and extended in the direction of the water flow. In the case of seepage due to the relatively large half-circumferential crack, the amount of water flowing out of the pipe was immediately excessive, the erosion damage to the soil was more serious, the upper covering soil fell off faster, and the soil volume was high. Consequently, the soil cavity formed a ground collapse without a lengthy and gradual development process, and the soil cavity was slightly oval.

(3) In the vertical damage experimental group, the width and height of the cavity formed in the two groups of experiments were similar. The cavities formed by 1 cm and 2 cm vertical cracks were 280 mm wide, 59 mm high and 270 mm wide and 58 mm high, respectively.

The cross-section of the pipe was broken, because of which there was water seepage from the pipe in the area surrounding the pipe, and the soil cavity resembled an inverted triangular shape (Figure 8c). The boundary of the soil cavity was not well defined, the overlying soil was close to the pipe, the sand bedding beneath the pipe had been heavily eroded, and cracks in the pipe could be seen through the cavity. Moreover, when the crack size exceeded a certain threshold, the pipe seeped out an excessive amount of water, the soil quickly hollowed out in a short time, and soil cavity development and ground collapse occurred in parallel. Although the soil cavity formed by the two types of cracks were about the same size, the former cavity size was slightly smaller than the latter, as the 2 cm vertical crack set formed the ground collapse slightly faster than the 1 cm vertical crack set, as shown in Table 1.

(4) From a comparison of the crack types, the vertical damage took only a short time for the pressure pipelines, because water at high speeds and pressures can quickly flow out and scour the soil around the pipelines; the cavity was significantly larger in area and degree of damage than the erosion cavity formed by circular cracks on the soil around the pipe.

3.2. Degree of Ground Collapse

The ground collapse phenomenon caused by pipe breakage often proceeds through the evolutionary process of "pipe breakage ⟶ soil erosion ⟶ cavity evolution ⟶ ground collapse". However, the varying development of the soil cavity at different crack sizes inevitably leads to variations in the degree of ground collapse.

By measuring and analyzing the ground settlement and ground damage area, Table 2 shows that as the crack size increases in the three sets of experiments, the ground settlement and the length of the ground settlement area increase as well, resulting in more serious ground collapse damage. In comparing the three types of cracks, it is clear that pipe breakage with vertical cracks causes more serious ground collapse than in the other two cases.

Table 2. Settlement and length of ground collapse.

Type of Cavity		Settlement above Cracks (mm)	Length of the Ground Settlement Area (mm)
Pipe wall perforation group	20 mm-diameter circular crack	13	335
	30 mm-diameter circular crack	18	402
	40 mm-diameter circular crack	17	435
Circumferential damage group	1/4 circumferential crack	12.7	339
	1/2 circumferential crack	20	490
Vertical damage group	1 cm vertical crack	31.6	434
	2 cm vertical crack	32.7	452

The impact of surge and spray breakage on ground collapse was simulated in the circumferential damage group. In this case, a quarter-circumferential circular crack means a surge leak and a half-circumferential circular crack means a spray leak. The ground settlement above cracks of these two types was 12.7 mm and 20 mm, respectively. The length of the ground settlement area of these types was 339 mm and 490 mm, respectively. The difference in the degree of damage to ground surfaces can clearly be seen.

Surge leaks make the soil around the pipe leak form a slender cavity. As the cavity exists at the interface between the sand layer and the experimental soil layer, the scouring effect on the overlying experimental soil is small, and the ground appears to exhibit moderate settlement. On the other hand, there is rapid flow out of the sand layer in the case of a spray leak case; therefore, the existence of a large cavity around the pipe further contributes to settlement and loss of the overlying experimental soil, resulting in significant ground settlement and a significant increase in the settlement area.

In the pipe wall perforation group, the ground collapse length extended with increasing crack size, from 335 mm with a 20 mm-diameter circular crack to 435 mm in the case of a 40 mm-diameter circular crack; the differences between the two adjacent groupswere 67 and 33 mm, respectively. Although the difference is not in this case as high as the 151 mm in the case of the circumferential crack group, it can be seen that the length of the ground collapse area increased significantly. Regarding the values for ground settlement above the cracks, there was not much change between circular cracks of 30 mm and 40 mm in diameter.

In the vertical damage group, the ground settlement values above the cracks caused by vertical cracks of 1 cm and 2 cm were 31.6 and 32.7 mm, respectively, and the respective lengths of the ground settlement area were 434 and 452 mm. Compared to the previous two sets of experiments, there was a significant reduction in the difference observed in the data. The difference in the vertical damage group in terms of ground settlement was only 1.1 mm, and the difference in the vertical damage group in terms of the length of the ground collapse area decreased to 18 mm.

As listed in Table 2, in the case of the 30 mm and 40 mm diameter circular cracks and the 1 cm and 2 cm vertical cracks, the difference in the settlement above the cracks and the difference in the length of the ground collapse settlement area were both significantly smaller than the differences in the other adjacent groups. When the crack was larger than a certain critical size, the hydraulic action in a short duration formed a rapid erosion cavity on the soil around the pipe, causing the ground to collapse. The ground settlement above the crack and the length of the ground collapse settlement area did not increase significantly, and a large amount of water flooded the ground.

The 3D laser scanning of the circumferential and vertical crack groups on the ground before and after the collapse and the post-processed contour images (Figure 9) can help more intuitively to compare the influences of the type and size of cracks on ground collapse. The blue, green, yellow, and orange colors represent the severe settlement area, general settlement area, general uplift area, and severe uplift area, respectively.

The contour image shows that the entire ground area of the model exhibited varying degrees of damage due to pipe breakage, with the settlement value at the center of the cracks, the settlement area, the height of the elevation at both ends of the ground, and the degree of ground damage all being significantly higher in the vertical damage group than in the circumferential damage group.

In the circumferential damage group, the quarter-circumferential damage was more toward the right end of the ground in terms of both ground settlement and ground uplift caused by the surge leak. The underground soil cavity formed in the surge leak was an elongated cavity to the right of the crack, resulting in the presence of a dehiscence area in the overlaying soil at the right end of the ground and the formation of ground settlement and uplift. Therefore, the half-circumferential damage was significantly greater than the quarter-circumferential damage in terms of ground settlement at the center of the crack, the height of the rise at the ends of the ground, and the settlement area caused by the spray leak.

In the vertical damage group, the ground collapse contours were extremely similar for both sizes, with no significant differences in the settlement values at the center of the crack, the settlement area, or the height of the rise at the ends of the ground surface. This further shows that when the crack is larger than a certain critical size, there is no significant change in the severity of the ground collapse caused by pipe breakage.

The more concentrated area of settlement in the vertical damage group compared to the circumferential damage group indicates that larger cracks cause more abrupt ground collapse due to the cavity. During the evolution of the ground collapse, the soil around the pipe erodes more rapidly, forming an underground cavity that rapidly erodes and expands. When the surrounding soil is not affected, the soil above the crack center then begins to collapse.

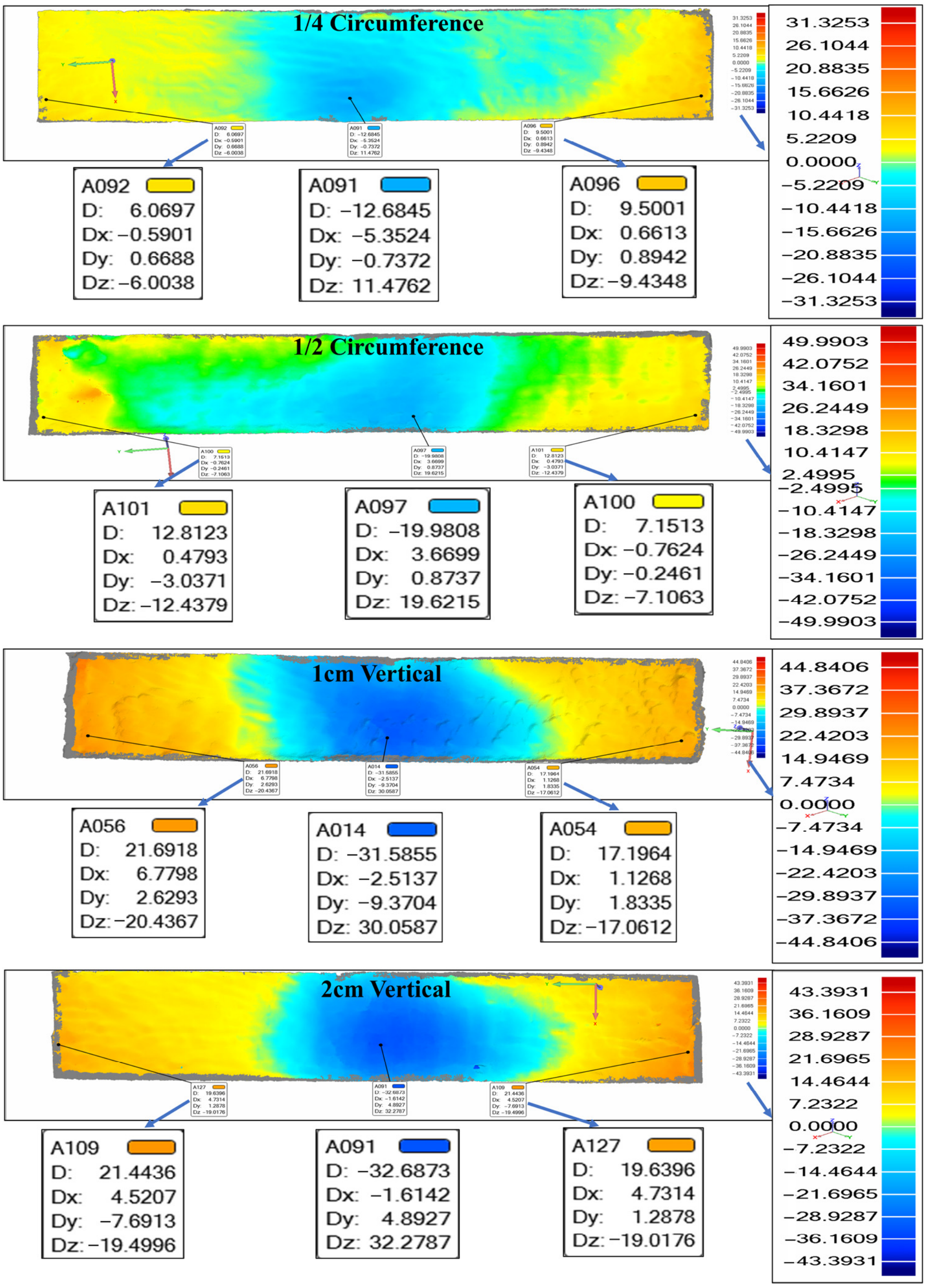

Figure 9. Three-dimensional laser scanning cloud images.

4. Conclusions

Through a water circulation pipeline breakage testing apparatus, the problem of ground collapse disaster caused by pipeline breakage was studied in this paper. A 3D laser scanning technology was applied in experimental data processing to analyze and compare the patterns of cavity evolution development and the degree of ground collapse after pipeline breakage under different crack types and sizes in the pipeline. The following conclusions can be drawn:

(1) By studying three sets of experimental processes, the evolution of ground collapse under the action of pipe breakage was obtained and divided into three stages: the soil erosion stage, the stable stage of cavity development, and the ground collapse stage.

(2) Among the different crack types, vertical damage had the worst damage and greatest impact on the degree of cavity development and ground collapse, with a short evolu-

tionary process and sudden formation of ground collapse. Across the different crack sizes, there was an increase in both the underground cavity size and the degree of ground collapse with increasing crack size, leading to an increase in the seepage force of the water in the pipeline; however, this increase was significantly lessened below a certain critical size.

(3) When studying the laws of cavity evolution and ground collapse development under the action of pipeline breakage, the two laws had a number of similarities, further revealing the significance of studying the evolution process of cavities for ground collapse prediction.

Due to limited indoor conditions, the experiment conducted in this study had certain shortcomings:

(1) The soil model box for the experiment was designed in the form of a semi-structure. Although silicone oil was applied to the walls of the model box, there are necessarily interaction forces between the soil in the model box and the inner walls of the model box, making it difficult to achieve the actual boundary conditions of the soil.
(2) In order to better realize the development process of the underground cavity and to achieve the effect of ground collapse, the loading and unloading method was applied in the experiment; however, this method does not fully conform to the normal formation pattern of underground cavities.
(3) The test box design was too small, and when the water pressure in the pipe was excessive, the water flowed to the ground from the boundary between the test box and the soil.

Author Contributions: F.T.: Conceptualization, Methodology, Writing—Review and Editing; W.T.: Writing—Original draft preparation; F.Y.: Investigation; X.Q.: Conceptualization, Supervision; Q.L.: Project administration; Z.H.: Data curation. All authors have read and agreed to the published version of the manuscript.

Funding: This research was funded by the National Natural Science Foundation of China (Grant Nos. 42277165 and 41920104007), the China Geological Survey Project Foundation (Grant No. DD20221734), and the Fundamental Research Funds for the Central Universities, China University of Geosciences (Wuhan) (Grant No. CUGCJ1821).

Data Availability Statement: Some or all data, models, or code that support the findings of this study are available from the corresponding author upon reasonable request.

Conflicts of Interest: The authors declare no conflict of interest.

References

1. Wang, X.W.; Xu, Y.S. Investigation on the phenomena and influence factors of urban ground collapse in China. *Nat. Hazards.* **2022**, *113*, 1–33. [CrossRef]
2. Song, G.C.; Ye, Y.C.; Liu, Q.R. Settlement causation and countermeasure analysis of urban roads in Beijing. *Urban Roads Bridges Flood Control* **2011**, 250–252. (In Chinese) [CrossRef]
3. Fu, D.; Cai, J.T.; Zhang, H. Numerical simulation of ground collapse caused by pipeline breakage in Shanghai. *Geotech. Eng. Tech.* **2018**, *32*, 189–193. (In Chinese)
4. Yan, F.; Qiu, W.; Sun, K.; Jiang, S.; Huang, H.; Hong, Y.; Hou, Z. Investigation of a large ground collapse, water inrush and mud outburst, and countermeasures during subway excavation in Qingdao: A case study. *Tunn. Undergr. Sp. Tech.* **2021**, *117*, 104127. [CrossRef]
5. Wang, J.A.; Shang, X.C.; Ma, H.T. Investigation of catastrophic ground collapse in Xingtai gypsum mines in China. *Int. J. Rock Mech. Min.* **2008**, *45*, 1480–1499. [CrossRef]
6. Shu, B.; Ma, B. Study of ground collapse induced by large-diameter horizontal directional drilling in a sand layer using numerical modeling. *Can. Geotech. J.* **2015**, *52*, 1562–1574. [CrossRef]
7. Phien-wej, N.; Giao, P.H.; Nutalaya, P. Land settlement in Bangkok, Thailand. *Eng. Geol.* **2006**, *82*, 187–201. [CrossRef]
8. Nguyen, Q.T. The main causes of land settlement in Ho Chi Minh City. *Procedia Eng.* **2016**, *142*, 334–341. [CrossRef]
9. Chaussard, E.; Amelung, F.; Abidin, H.; Hong, S.H. Sinking cities in Indonesia: ALOS PALSAR detects rapid settlement due to groundwater and gas extraction. *Remote Sens. Environ.* **2013**, *128*, 150–161. [CrossRef]
10. Rahnema, H.; Mirasi, S. Seismic and geotechnical study of land subsidence and vulnerability of rural buildings. *Int. J. Geosci.* **2012**, *3*, 878–884. [CrossRef]

11. Rahnema, H.; Mirassi, S. Study of land subsidence around the city of Shiraz. *Sci. Iran. Trans. A Civ. Eng.* **2016**, *23*, 882–895.
12. Liu, C.M.; Wei, H.Y.; Zhang, H.J. Relationship between urban road collapse and underground pipeline. *Urban Geotech. Invest. Surv.* **2020**, 183–187. (In Chinese) [CrossRef]
13. Hu, Y.H.; Bai, Y.C.; Xu, H.J. Analysis of reasons for urban road collapse and prevention and control countermeasures in recent decade of China. *Highways* **2016**, *61*, 130–135. (In Chinese)
14. Wang, Y.L.; Lu, Y. CFD-DEM joint calculation and simulation of disaster mechanism of pavement collapse caused by pipeline breakage in urban areas. *J. Civ. Environ. Eng.* **2021**, *43*, 60–67. (In Chinese)
15. Zhou, H.T.; Liu, C.Q.; Wang, G.H.; Kang, K.; Liu, Y.H. Study on drilling ground collapse induced by groundwater flow and prevention based on a coupled CFD-DEM method. *KSCE J. Civ. Eng.* **2022**, *26*, 2112–2125. [CrossRef]
16. Ben-Mansour, R.; Habib, M.A.; Khalifa, A.; Youcef-Toumi, K.; Chatzigeorgiou, D. Computational fluid dynamic simulation of small leaks in water pipelines for direct leak pressure transduction. *Comput. Fluids* **2012**, *57*, 110–123. [CrossRef]
17. Peche, A.; Graf, T.; Fuchs, L.; Neuweiler, I. A coupled approach for the three-dimensional simulation of pipe breakage in variably saturated soil. *J. Hydrol.* **2017**, *555*, 569–585. [CrossRef]
18. Lau, P.K.W.; Cheung, B.W.Y.; Lai, W.W.L.; Sham, J.F.C. Characterizing pipe breakage with a combination of GPR wave velocity algorithms. *Tunn. Undergr. Sp. Tech.* **2021**, *109*, 103740.
19. Qi, G.; Wang, Z.; Chen, Y.; Zhu, C.; Ren, D.; Tian, T.; Yang, F. Analysis of instability mechanism and induced cause of urban pavement in Xining City, China. *Adv. Mater. Sci. Eng.* **2022**, *2022*, 3365402. [CrossRef]
20. Al-Halbouni, D.; Holohan, E.P.; Taheri, A.; Schöpfer, M.P.J.; Emam, S.; Dahm, T. Geomechanical modelling of sinkcavity development using distinct elements: Model verification for a single void space and application to the Dead Sea area. *Solid Earth* **2018**, *9*, 1341–1373. [CrossRef]
21. Rahnema, H.; Mirassi, S.; Dal Moro, G. Cavity effect on Rayleigh wave dispersionand P-wave refraction. *Earthq. Eng. Eng. Vib.* **2021**, *20*, 79–88. [CrossRef]
22. Mirassi, S.; Rahnema, H. Deep cavity detection using propagation of seismic waves in homogenous halfspace and layered soil media. *Asian J. Civ. Eng.* **2020**, *21*, 1431–1441. [CrossRef]
23. Tang, Y.; Chan, D.H.; Zhu, D.Z. A coupled discrete element model for the simulation of soil and water flow through an orifice. *Int. J. Numer. Anal. Met.* **2017**, *41*, 1477–1493. [CrossRef]
24. Cui, X.L.; Tao, G.L.; Li, J. Experiment and numerical simulation on seepage failure of sand caused by breakage of underground water pipe. *IOP Conf. Ser. Earth Env. Sci.* **2018**, *153*, 032033. [CrossRef]
25. Indiketiya, S.; Jegatheesan, P.; Rajeev, P. Evaluation of defective sewer pipe–induced internal erosion and associated ground deformation using laboratory model test. *Can. Geotech. J.* **2017**, *54*, 1184–1195. [CrossRef]
26. Nazari SGholami, R.; Mirassi, S. Laboratory evaluation of Scour rate and energy dissipation in Gabion Stepped Weirs with considering the effect of Discharge and tail water depth. *J. Appl. Sci. Agric.* **2014**, *9*, 1424–1439.
27. Ali, H.; Choi, J. Risk prediction of sinkcavity occurrence for different underground soil curves due to breakage from underground sewer and water pipelines. *Sustainability* **2019**, *12*, 310. [CrossRef]